Field emission enhancement in ultrananocrystalline diamond films by in situ heating during single or multienergy ion implantation processes

P. T. Joseph, N. H. Tai, C. H. Chen, H. Niu, H. F. Cheng et al.

Related Articles

Additional information on J. Appl. Phys.

Field emission enhancement in ultrananocrystalline diamond films by *in situ* heating during single or multienergy ion implantation processes

P. T. Joseph,[1] N. H. Tai,[1,a)] C. H. Chen,[2] H. Niu,[2] H. F. Cheng,[3] U. A. Palnitkar,[4] and I. N. Lin[4,b)]

[1]*Department of Materials Science and Engineering, National Tsing-Hua University, Taiwan 300, Republic of China*
[2]*Nuclear Science and Technology Development Center, National Tsing-Hua University, Taiwan 300, Republic of China*
[3]*Department of Physics, National Taiwan Normal University, Taiwan 116, Republic of China*
[4]*Department of Physics, Tamkang University, Tamsui 251, Taiwan, Republic of China*

The single or multienergy nitrogen (N) ion implantation (MENII) processes with a dose (4×10^{14} ions/cm^2) just below the critical dose (1×10^{15} ions/cm^2) for the structural transformation of ultrananocrystalline diamond (UNCD) films were observed to significantly improve the electron field emission (EFE) properties. The single energy N ion implantation at 300 °C has shown better field emission properties with turn-on field (E_0) of 7.1 V/μm, as compared to room temperature implanted sample at similar conditions ($E_0 = 8.0$ V/μm) or the pristine UNCD film ($E_0 = 13.9$ V/μm). On the other hand, the MENII with a specific sequence of implantation pronouncedly showed different effect on altering the EFE properties for UNCD films, and the implantation at 300 °C further enhanced the EFE behavior. The best EFE characteristics achieved for the UNCD film treated with the implantation process are $E_0 = 4.5$ V/μm and current density of (J_e) = 2.0 mA/cm^2 (at 24.5 V/μm). The prime factors for improving the EFE properties are presumed to be the grain boundary incorporation and activation of the implanted N and the healing of induced defects, which are explained based on surface charge transfer doping mechanism. © *2009 American Institute of Physics*. [DOI: 10.1063/1.3152790]

I. INTRODUCTION

Diamond films electron field emission (EFE) properties, which are possibly due to the negative electron affinity,[1,2] along with many other excellent properties, such as mechanical stability, chemical inertness, high thermal conductivity, etc.,[1–5] make an ideal candidate for cold cathode emission display applications. Moreover, ultrananocrystalline diamond (UNCD) films with grain size of 3–5 nm and sp^2 rich grain boundaries can show better EFE characteristics as compared to diamond films with micron-sized grains.[6] The highly reproducible EFE properties and planar emitting surface of UNCD films could be advantageous over other field emitting materials, such as sharp tips that require complicated fabrication processes and carbon nanotubes that often face the problem of reproducing similar EFE characteristics. Therefore, UNCD films are fabulous and potential candidates for cold cathode field emitters and vacuum nanoelectronic devices. In addition, tuning the electronic properties with doping of particular species [such as boron (B), phosphorous (P), or nitrogen (N)][3–5] or engineering of nanostructures with the ion irradiation process opens up the possibility of this material for electronic applications.[7–10]

The ion implantation (or irradiation) process has been a common technique to engineer the structure, incorporate dopant species into a specific depth, and thereby improve the diverse properties of different materials. It is known that irradiation of energetic particles with solids can create defects and deteriorate the materials. A thermal postimplantation annealing process is required to eliminate the defects and sometimes activate the dopants to have useful effects. Reports show the better annealing effects of low energy ion-implanted diamond with the irradiation of higher energy (MeV) ions than the conventional postimplantation annealing process.[11] The occurrence of severe damage during ion implantation onto carbon materials can be minimized by performing the ion implantation at or above 300 °C, which can effectively anneal out irradiation-induced damages through dangling bond saturation.[12] The recent reports show that the ion implantation on nanostructures can have beneficial effects especially when integrated with heat treatment, and this method can be used to tailor the structure and properties of nanosystems with high precision.[9] Furthermore, ion implantation can be used to modify the mechanical, electronic, and even magnetic properties of carbon materials.[7–10] In case of diamond films, the enhancement in field emission properties due to ion implantation introduced defects and the removal of defects as well as enhanced emission properties with the postimplantation annealing process have been reported.[13] Previously we have reported that the single energy N ion implantation (SENII) process combined with the postimplantation annealing process could improve the EFE properties of UNCD films.[8] However, large proportions of defects were also induced during the ion implantation process, which impedes the understanding on whether the presence of defects or the doping of N ions improved the EFE behavior.

a)Electronic mail: nhtai@mse.nthu.edu.tw.
b)Electronic mail: inanlin@mail.tku.edu.tw.

In this study, we specially designed the SENII as well as separate multienergy N ion implantation (MENII) experiments for understanding the genuine factors that enhanced the EFE properties of UNCD films. The implantation processes on UNCD films were carried out with a dose just below the critical dose[7–9] (10^{15} ions/cm²) to incorporate maximum dopant species into the film by preventing the formation of irreversible structural damages in the films. We herein report that an *in situ* heating (at 300 °C) during the ion implantation process can further improve the EFE properties of UNCD films. Based on the x-ray photoelectron spectroscopy (XPS) C 1*s* binding energy peak shifts of different N-ion-implanted UNCD films, we show that defect formation during the implantation of single energy ions, their subsequent self-annealing with the implantation of higher energy ions (for MENII), and *in situ* healing of defects by the implantation at an elevated temperature result in a complex evolution of field emission properties. The improved emission properties of UNCD films are discussed based on the defect formation or healing, possible incorporation of N ions into the grain boundaries, activation of the incorporated N ions, and a transfer doping mechanism.

II. EXPERIMENTAL METHODS

UNCD films were grown on *n*-type silicon substrates in a microwave plasma enhanced chemical vapor deposition (IPLAS-Cyrannus) system. The substrates were preseeded by ultrasonication in a solution containing nanodiamond and titanium powders for 45 min. UNCD was grown in $CH_4(1\%)/Ar$ plasma with gas flow rate of 100 (SCCM denotes standard cubic centimeter per minute at STP), microwave power of 1.2 kW, and at a pressure of 120 Torr for 3 h. No substrate heating was used prior to or during the growth of UNCD films. The bonding nature of UNCD film was examined using near edge x-ray absorption spectroscope (NEXAFS), and the microstructure of UNCD film was examined using transmission electron microscope (TEM, JOEL-2100).

Nitrogen (N) ion implantations into UNCD films were carried out in HVEE500KV-implantor at room temperature and at 300 °C with a pressure below 5×10^{-6} Torr. The TRIM software[14] was used to evaluate the trajectory of ions and to estimate the critical dose for transforming the sp^3- to the sp^2-bonds.[15] For the SENII (100 keV) processes the ion dose was 4×10^{14} ions/cm². For the MENII processes, four different ion energies (50, 100, 150, and 200 keV) were chosen for implantation, which were carried out either from low energy to high-energy or in a reverse sequence. The ion dose for each energy was 1×10^{14} ions/cm² and resulted in a total dose of 4×10^{14} ions/cm², which was controlled at a level lower than the critical dose[7–9] (1×10^{15} ions/cm²) to avoid the induction of irreversible structural damage. The TRIM calculation indicates that the approximate penetration depth is 255 nm for 200 keV, 200 nm for 150 keV, 140 nm for 100 keV, and 75 nm for 50 keV ions. For simplicity, single energy ion-implanted sample was designated as S_{100}, and the multienergy ion-implanted samples were designated according to the initial energy of implanted ions, such as

M_{200} for samples first ion-implanted with high-energy (200 keV) and M_{50} for samples first ion implanted with low energy (50 keV) ions. It has to be noted that our previous studies showed that the thermal annealing effect on ion-implanted UNCD was beneficial to improve the field emission properties.[8] This behavior is much different from the thermal annealing effect on ion-irradiated diamond films, where the enhanced EFE properties were eliminated after the annealing process.[12] In conjunction with that observation, the same set of room temperature N ion implantation experiments was carried out at elevated temperature. The S_{100}, M_{200}, and M_{50} N ion implantation processes were performed at 300 °C to investigate the *in situ* annealing effects during the implantation processes on the EFE properties of UNCD films, and the samples were designated as S'_{100}, M'_{200}, and M'_{50}, respectively.

The UNCD films before and after ion implantation were characterized using Raman spectroscopy, secondary ion mass spectroscopy (SIMS; Cameca, IMS-4f), and XPS (PHI, 1600). The direct observation of secondary ions of N using SIMS is difficult due to the interference of hydrocarbon masses for positive N and lack of stable negative N,[16] the CN depth profile of 26.003 amu (negative polarity mode) was used to monitor the presence of nitrogen in UNCD films. Only the analysis of C 1*s* peak is reported since no significant N 1*s* peak was observed during the XPS studies. Field emission characteristics of the films were measured with Keithley 237 electrometer.[17] For the EFE measurement, a molybdenum (Mo) tip with a diameter of 2 mm was used as anode. The distance between anode and cathode was measured with a digital micrometer, which also was ensured with an optical microscope. The turn-on field is designated as the electric field required for a current density of 0.1 $\mu A/cm^2$.

III. RESULTS AND DISCUSSION

Raman spectrum of UNCD film [Fig. 1(a)] shows typical nanodiamond characteristics, such as *D*-band (~ 1330 cm⁻¹), *G*-band (~ 1540 cm⁻¹), and *G'*-band (~ 1590 cm⁻¹), originating from defect, graphitic structure, and nanographitic structure, respectively, in the film. The v_1-band (~ 1140 cm⁻¹) and v_3-band (~ 1460 cm⁻¹) represent transpolyacetylene along the grain boundaries.[18] XPS spectrum of pristine UNCD [inset of Fig. 1(a)] reveals the C 1*s* peak at 285.4 eV, which is near the typical C–C binding energy for diamond,[19] indicating no considerable surface charging or oxidation on these films. Typical NEXAFS spectrum shown in Fig. 1(b) indicates the presence of sharp rise at 289.7 eV (σ^*-band), inferring the sp^3-bonded nature of UNCD films,[20] and TEM image [inset of Fig. 1(b)] shows that the grains are typically around 5 nm.

To investigate specifically, the incorporation of N into the UNCD films, the penetration depth of different energies of N ions, and the SIMS CN⁻ depth profile of pristine UNCD as well as separately prepared 100 and 200 keV N-ion-implanted UNCD films were measured, and the results are shown in Figs. 2(a)–2(c). It can be seen from Figs. 2(b) and 2(c) that the implantation of single energy ions could create a specific N-implanted region in the depth profile. The TRIM
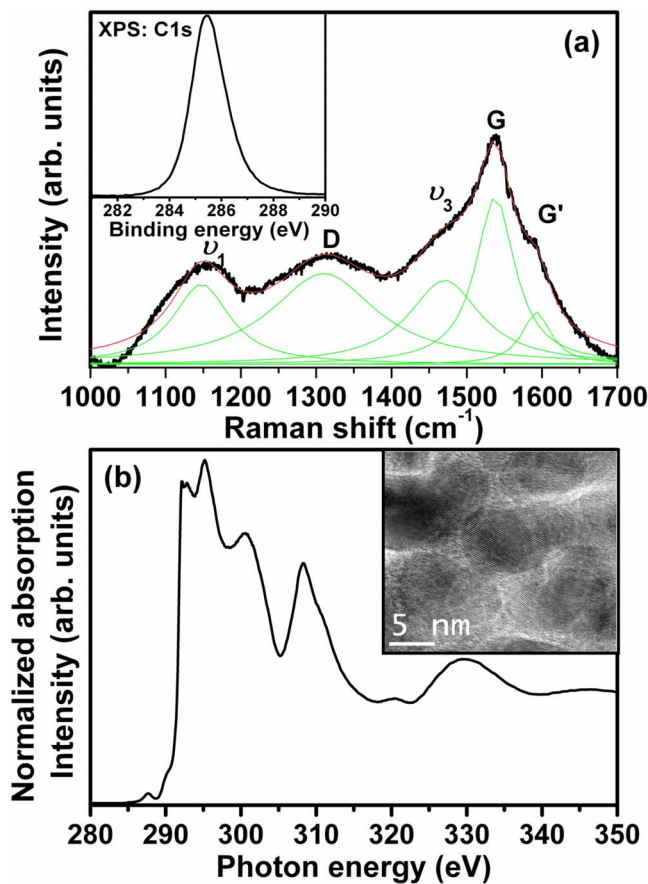
FIG. 1. (Color online) (a) Typical Raman spectrum of UNCD film with XPS spectrum shown as inset and (b) typical NEXAFS spectrum of UNCD film with the HRTEM image shown as inset.
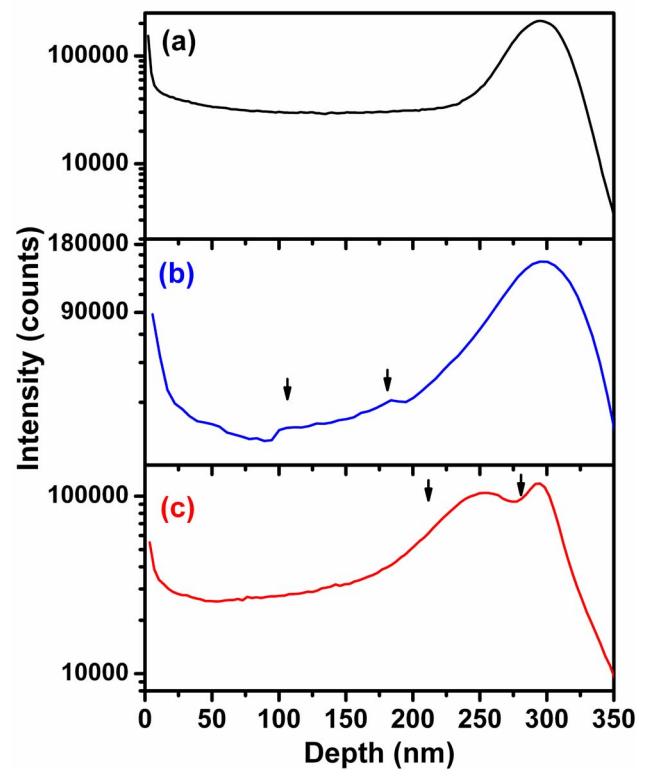

FIG. 2. (Color online) SIMS CN-depth profile of UNCD films before and after the N ion implantation at room temperature. (a) Pristine UNCD film, (b) 100 keV N-ion-implanted UNCD film, and (c) 200 keV N-ion-implanted UNCD film. The arrows in (b) and (c) show the region where implanted N ions are accumulated. It is presumably where the ions reach their end of trajectories. The depth of the implanted region increased with the energy of implanted ions.

studies for the 100 and 200 keV ion implantation onto UNCD films also show that the ions with different energies can reach different penetration depths (figures not shown). Therefore, it is imperative to design an experiment to implant the N ions throughout the films by implanting the ions with different energies, which is expected to improve the uniformity of N in the film.

Figures 3 and 4 show the field emission property of UNCD films before and after the N ion implantation (SENII or MENII) processes carried out at room temperature and at 300 °C, respectively. The EFE properties including turn-on field (E_0) and current density (J_e) were extracted and are listed in Table I. The electron emission of the pristine UNCD film can be turned on at $(E_0)_{UNCD}=13.9$ V/μm, achieving an EFE current density of $(J_e)_{UNCD}=0.26$ mA/cm^2 at an applied field of 42.5 V/μm. The effect of room temperature N ion implantation (SENII or MENII) processes on the field emission properties of UNCD films (Fig. 3) will be discussed first. The turn-on field E_0 of pristine UNCD film is reduced to about 8.0 V/μm after the SENII process (for S_{100} film) and reached the EFE current density of $(J_e)_{S_{100}}$ =0.7 mA/cm^2 at the applied field of 42.5 V/μm.

For MENII processes, the sequence of ion implantation imposes marked effect on the EFE properties of UNCD films. The ion implantation started with high-energy N ions only moderately improved the EFE properties, viz., turn-on field decreased to $(E_0)_{M_{200}}=9.0$ V/μm and emission current

density at $V_a=42.5$ V/μm applied field increased to $(J_e)_{M_{200}}=0.5$ mA/cm^2. Additionally, the emission current density fluctuates, indicating that the surface of M_{200} film is not very stable for field emission. In contrast, ion implantation started with low energy N ions (M_{50}) not only significantly enhanced the EFE characteristics but also rendered the EFE behavior very stable, i.e., the emission current density
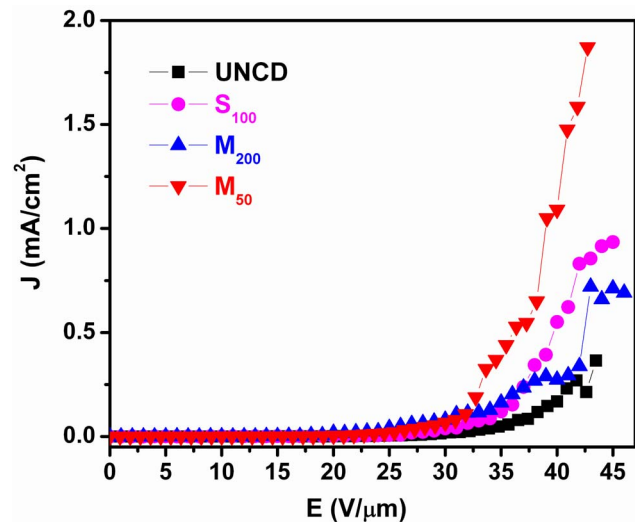

FIG. 3. (Color online) Field emission data of UNCD films before and after the SENII and MENII processes carried out at room temperature.
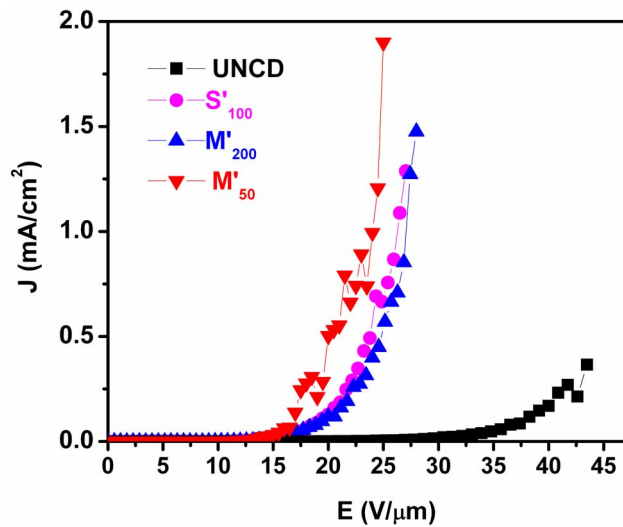
FIG. 4. (Color online) Field emission data of UNCD films before and after the SENII and MENII processes carried out at 300 °C.
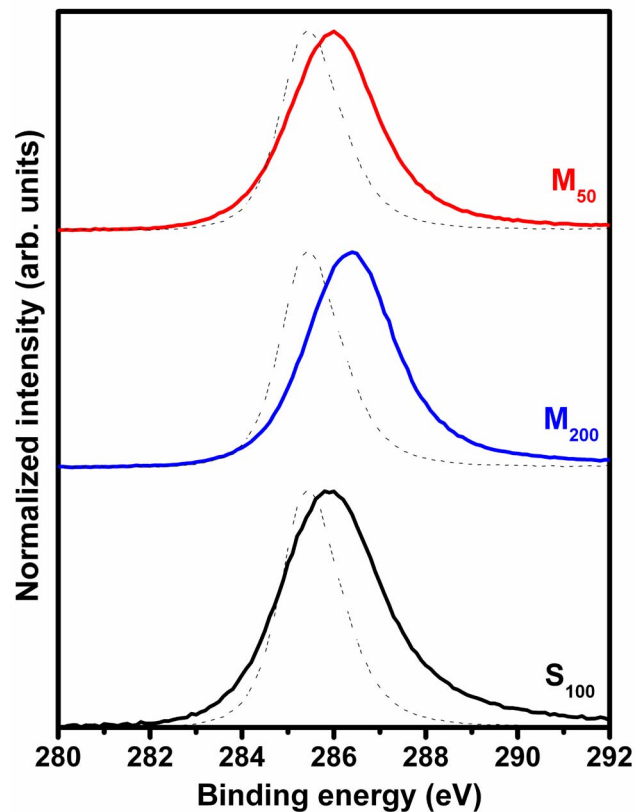

FIG. 5. (Color online) XPS C 1s peak shift of UNCD films after the SENII and MENII processes carried out at room temperature. The dotted line is the C 1s peak of pristine UNCD film.

increased with the applied fields smoothly. The turn-on field decreased further to $(E_0)_{M_{50}}=7.3$ V/μm, and the EFE current density increased dramatically to $(J_e)_{M_{50}}=2.0$ mA/cm^2 at the applied field of 42.5 V/μm. The superior EFE properties for the M_{50} film to those for the M_{200} film is possibly due to the thermal annealing effect resulting from the interaction of subsequently implanted energetic N ions with the lattices.[11] However, it should be noted that the emission mechanism is not well understood yet. The possible emission mechanism for ion-implanted samples is due to the formation of multiple conduction paths with more than one energy level owing to grain boundary sp^2 phase, incorporated nitrogen, and defects,[21] which are enhancing the EFE properties.

To understand how the N ion implantation processes affect the EFE properties of UNCD films, the structure and surface properties of the ion-implanted films were examined using Raman spectroscopy and XPS, respectively. Raman spectra of the films are essentially not altered due to the different ion implantation processes (figures not shown), which confirm that the dose used in these experiments is below the critical dose of 10^{15} ions/cm^2 and could not generate irreversible structural damage on UNCD films. Alternately, the normalized XPS spectra in Fig. 5 show that the room temperature SENII or MENII processes markedly modify the surface characteristics of UNCD films. For comparison, the XPS C 1s spectrum of pristine UNCD is also included as dotted line, which is shown in the figures. As

listed in Table I, the C 1s peak shifts to 285.9 eV for the S_{100} film $[(\Delta f)_{S_{100}}=0.5$ eV$]$, 286.4 eV for the M_{200} film $[(\Delta f)_{M_{200}}=1.0$ eV$]$, and 286.0 eV for the M_{50} film $[(\Delta f)_{M_{50}}=0.6$ eV$]$, where (Δf) is the blueshift of C 1s peak with respect to that of the pristine UNCD film. These results imply that the proportion of charge trapping centers, which are presumably the atomic defects, increased due to energetic ions bombardment. Furthermore, the implantation of N ions into UNCD film can cause the removal of H from the film,[8] exposing the dangling bonds, which also possibly contribute for the C 1s blueshift.[22,23] Higher C 1s blueshift for M_{200} film suggests that it contains more abundant atomic defects or defect complexes as compared with the S_{100} and the M_{50} films. The defects induced variation in full width at half maximum (FWHM) of C 1s spectra[12] is also evident from the figures, which further support the above arguments.

While the primary interaction of implanted ions with the

TABLE I. The details of ion energies used in the SENII or MENII experiment and the properties of UNCD films before and after the implantation processes.

	UNCD (pristine)	N-ion-implanted at 25 °C			N-ion-implanted at 300 °C		
		S_{100}	M_{200}	M_{50}	S'_{100}	M'_{200}	M'_{50}
E_0 (V/μm) [a]	13.9	8.0	9.0	7.3	7.1	6.9	4.5
J_e (mA/cm^2 @ V/μm) [b]	0.26 @ 42.5	0.7 @ 42.5	0.5 @ 42.5	2.0 @ 42.5	2.0 @ 26	2.0 @ 27	2.0 @ 24.5
C 1s (eV) [c]	285.4	285.9	286.4	286.0	285.7	285.5	285.5

[a]Turn-on field for electron emission.
[b]Current density at specific applied field (V_a).
[c]XPS C–C binding energy peak position.

lattice is to induce atomic defects, they could also heal of the atomic defects existing in their path due to the thermal annealing effect.[9,11] For M_{200} sample, penetration depth of N ions decreases from 255 nm for 200 keV ions to 75 nm for 50 keV ions such that atomic defects induced by 200 keV ions could not be annealed out by the subsequently irradiated 150 keV ions, etc. The defects induced in each step are thus accumulated and possibly create defect complexes or even form clusters of dopant species. On the contrary, for M_{50} sample, the penetration depth of ions increases with increasing ion energies, i.e., 75, 140, 200, and 255 nm for 50, 100, 150, and 200 keV ions, respectively. The defects induced by the first three steps (50, 100, and 150 keV N ions) can possibly be healed by the subsequently implanted ions in the last step (200 keV N ions). Only the atomic defects induced by 200 keV N ions remain in the depth around 255 nm beneath the surface. The proportions of atomic defects, defect complexes, clusters of carbon, or dopant species that remain in M_{200} films are therefore higher than that residing in the M_{50} films, and the removal of H from the near surface is possibly contributing for the higher blueshift of the C 1s peak (Fig. 3).[8,22,23]

Although such a defect model correlates very well with C 1s blueshift phenomenon, it cannot be accounted for the phenomenon that the M_{50} film possesses superior EFE properties than the M_{200} film, as the defects are fewer in this film. Apparently, the modified EFE properties for the UNCD films are not because of the proportion of induced defects. The N ions residing in UNCD film must also be contributed to the process for enhancing the EFE properties. It should be noted that most of the implanted N ions remain in the UNCD film due to the low kinetic energy, which is also proved from the SIMS results [Figs. 2(b) and 2(c)]. The N ions, in principle, stay in the same region where the atomic defects reside, as the implanted ions causing displacement of lattice atoms are mostly at the end of their trajectories. Therefore, the MENII processes distribute the N ions more uniformly over the films than the case where only single energy ions were implanted. The N ions gather in regions nearly 75 nm from the film surface for 50 keV N ions and 150 nm for 100 keV, 225 nm for 150 keV, and 300 nm for 200 keV. The distribution of N ions is considered similar, which is regardless of the sequence of ion implantation processes. The superior EFE properties of M_{50} film imply that the low energy N ions implanted in this film are activated by the self-annealing with the subsequent implantation of higher energy N ions and thus more efficiently converted the films into semiconducting.

Previous reports[24,25] indicated that the N ions incorporated into UNCD films via the growth process lead to the accumulation of N into the grain boundary regions and then create *n*-type conductivity. Here, we suspect that the grain boundary incorporation of N ions converts the N-ion-implanted UNCD films into semiconducting films via the charge transfer process.[26,27] For the M_{200} films, the N ions coexist with the atomic defects and convert less efficiently in the "transfer doping" of UNCD grains. In contrast, for the M_{50} film, the defects are self-annealed or healed by the sub-

sequently implanted N ions, also activate more N ions reside at the grain boundaries, and efficiently convert UNCD grains via the transfer doping process.

The aforementioned results indicate that the MENII process with the implantation of higher energy ions after low energy ions considerably improved the EFE properties of UNCD films. The prime factor is the uniform distribution of N ions into the grain boundaries of UNCD and their activation by the self-annealing process. These processes further can be tuned to improve uniformity of the ion distribution and thereby enhance the EFE properties of UNCD. For this purpose, the ion implantation was carried out at an elevated temperature. It is expected that the ion bombardment induced defects possibly healed *in situ*, and diffusivity of N ions into the grain boundaries can be enhanced such that the uniformity in the distribution of N ions in UNCD can be improved.

In comparison with the SENII or MENII processes carried out at room temperature, the ion-implanted UNCD films at 300 °C have shown tremendously enhanced EFE properties (Fig. 4). The field emission data of pristine UNCD film also are plotted in the figure to clearly show the effect of these novel implantation processes. The detailed properties are summarized in Table I. The UNCD film after SENII process at 300 °C showed a turn-on field of $(E_0)_{S'_{100}}$ =7.1 V/μm and achieved a EFE current density of around 2.0 mA/cm^2 at an applied field of 26 V/μm. The MENII process carried out at 300 °C with high-energy ion-implanted first (dose for each energy of $\sim$1 $\times 10^{14}$ ions/cm^2) slightly reduced the turn-on field to $(E_0)_{M'_{200}}$=6.9 V/μm, and the EFE current density reached around 2.0 mA/cm^2 at an applied field of 27 V/μm. Interestingly, for the MENII process that started with 50 keV ions and followed by 100, 150, and 200 keV ions (dose for each energy of $\sim$1$\times 10^{14}$ ions/cm^2), M'_{50} lowered markedly the turn-on field to $(E_0)_{M'_{50}}$=4.5 V/μm and achieved a current density of 2.0 mA/cm^2 at a low applied field of 24.5 V/μm. It should be noted that the current density is only around $(J_e)_{M_{50}}\sim$0.05 mA/cm^2 at this applied field for the samples implanted at room temperature.

Similar to the previous set, the Raman investigation shows no significant variation in the structure after ion implantation at 300 °C (figures not shown). The XPS spectra of ion-implanted samples processed at 300 °C are shown in Fig. 6. It is interesting to observe that the blueshift of the C 1s peak are considerably lowered for ion-implanted samples at 300 °C as compared to room temperature implanted samples. However, a slight blueshift for C 1s peak is observed for S'_{100} film [$(\Delta f)_{S'_{100}}$=0.2 eV], which suggests that there still exist some defect centers that probably occurred due to the unavoidable removal of H from the film during the implantation process. The UNCD films after the MENII processes with *in situ* heating show almost no blueshift for their C 1s peak [both $(\Delta f)_{M'_{200}}$ and $(\Delta f)_{M'_{50}}$ are equal to 0.1 eV], inferring that atomic defects induced by ion irradiation are effectively healed. The insignificant C 1s peak blueshift for the M'_{200} and M'_{50} films is perhaps due to the saturation of dangling bonds[13] that eliminated the defects, thus diminished the surface charging effects, and effectively incorporated the
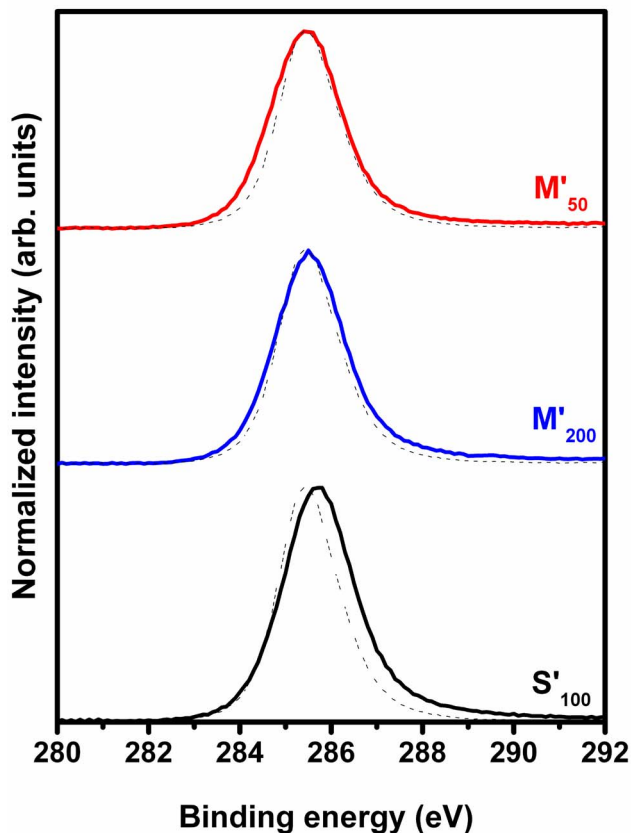
FIG. 6. (Color online) XPS C 1*s* peak shift of UNCD films after the SENII and MENII processes carried out at 300 °C. The dotted line is the C 1*s* peak of pristine UNCD film.

N ions into grain boundaries. The *in situ* elimination of defects due to the implantation process at 300 °C is further supported by the insignificant variation in the FWHM of C 1*s* spectra.[12]

In addition to the *in situ* elimination of point defects, the major effects of *in situ* heating during the ion implantation process are the uniform incorporation of N ions into UNCD films, presumably along the grain boundaries, and the activation of them. For M'_{50} film, in addition to the *in situ* annealing effect, the self-annealing due to the implantation of high-energy ions provides a "double-annealing" effect.[9,11] This double-annealing effect perhaps helps to incorporate maximum N ions into the UNCD grain boundaries and activate them to provide beneficial effect for enhancing the field emission properties. The observations suggest that the enhancement in EFE properties due to double-annealing effect of N-ion-implanted UNCD is not the conversion of sp^3-bonded carbons into sp^2-bonded ones. The plausible mechanism is that the N ions residing at grain boundary can efficiently convert the UNCD grains into semiconducting via the transfer doping process,[26,27] enhancing the EFE behavior.

Since the dose chosen in this study was very high, therefore for the room temperature ion implantations, the formation of defects was expected. The formed defects or defect complexes contributed significantly to the blueshift of C 1*s* peak. Furthermore, the annealing effect of high-energy ions after the low energy ion implantation was also beneficial to heal the defects and activate the implanted N ions to some extent, which are expected to contribute for the enhanced EFE properties. This suggests that effective doping of implanted species can be achieved while doing the implantation at an elevated temperature above 300 °C and thus improve the field emission properties as compared to room temperature implanted ones. The primary factors that promote the emission properties are uniform implantation of N ions into the grain boundaries of UNCD film and successful activation with the double-annealing effect. In other words, the multi-energy N ions implantation with higher energy ion implantation after the implantation of low energy ions effectively improves the EFE properties of UNCD via the enhancement in transfer doping process.

IV. CONCLUSIONS

Enhancement in the field emission properties of UNCD films with the SENII or MENII processes is reported. The structure of UNCD was kept intact after the implantation of N ions with the total dose of 4×10^{14} ions/cm^2. The multi-energy ion-implanted UNCD film with implanting higher energy ions after the implantation of low energy ions at an elevated temperature of 300 °C has shown better field emission properties as compared to room temperature implanted films. The M'_{50} film (MENII process at 300 °C) has shown the best field emission properties ($E_0 = 4.5$ V/μm) as compared to other samples, which is probably due to the uniform incorporation of N ions into the grain boundaries of UNCD film, the successful activation of grain boundary N ions by the double-annealing effect, and the enhanced surface charge transfer doping mechanism.

[1]E. Wilks and J. Wilks, *Properties and Applications of Diamond* (Butterworth-Heinemann, Oxford, 1991).
[2]P. Reichart, G. Datzmann, A. Hauptner, R. Hertenberger, C. Wild, and G. Dollinger, Science **306**, 1537 (2004).
[3]K. Okano, S. Koizumi, S. R. P. Silva, and G. A. J. Amaratunga, Nature (London) **381**, 140 (1996).
[4]G. A. J. Amaratunga and S. R. P. Silva, Appl. Phys. Lett. **68**, 2529 (1996).
[5]S. Koizumi, K. Watanabe, M. Hasegawa, and H. Kanda, Science **292**, 1899 (2001).
[6]W. Zhu, G. P. Kochanski, and S. Jin, Science **282**, 1471 (1998).
[7]S. Talapatra, J. Y. Cheng, N. Chakrapani, S. Trasobares, A. Cao, R. Vajtai, M. B. Huang, and P. M. Ajayan, Nanotechnology **17**, 305 (2006).
[8]P. T. Joseph, N. H. Tai, Y. C. Lee, H. Niu, W. F. Pong, and I. N. Lin, J. Appl. Phys. **103**, 043720 (2008).
[9]A. V. Krasheninnikov and F. Banhart, Nature Mater. **6**, 723 (2007).
[10]S. Talapatra, P. G. Ganesan, T. Kim, R. Vajtai, M. Huang, M. Shima, G. Ramanath, D. Srivastava, S. C. Deevi, and P. M. Ajayan, Phys. Rev. Lett. **95**, 097201 (2005).
[11]J. Nakata, Phys. Rev. B **60**, 2747 (1999).
[12]A. V. Krasheninnikov, K. Nordlund, and J. Keinonen, Phys. Rev. B **65**, 165423 (2002).
[13]W. Zhu, G. P. Kochanski, S. Jin, L. Seibles, D. C. Jacobson, M. McCormack, and A. E. White, Appl. Phys. Lett. **67**, 1157 (1995).
[14]J. F. Zielger, J. P. Biersack, and U. Littmark, *The Stopping and Range of Ions in Solids* (Pergamon, New York, 1985).
[15]K. C. Walter, H. H. Kung, and C. J. Maggiore, Appl. Phys. Lett. **71**, 1320 (1997).
[16]D. Zhou, A. R. Krauss, L. C. Qin, T. G. McCauley, D. M. Gruen, T. D.

Corrigan, and R. P. H. Chang, J. Appl. Phys. **82**, 4546 (1997).

[17] Y. C. Lee, S. J. Lin, I. N. Lin, and H. F. Cheng, J. Appl. Phys. **97**, 054310 (2005).

[18] A. C. Ferrari and J. Robertson, Phys. Rev. B **63**, 121405 (2001).

[19] F. Le Normand, J. Hommet, T. Szorenyi, C. Fuchs, and E. Forgarassy, Phys. Rev. B **64**, 235416 (2001).

[20] X. Xiao, J. Birrel, J. E. Gerbi, O. Auciello, and J. A. Carlisle, J. Appl. Phys. **96**, 2232 (2004).

[21] T. Sharda and S. Bhattacharyya, *Encyclopedia of Nanoscience and Nanotechnology*, edited by H. S. Nalwa (American Scientific Publishers, California, 2003).

[22] Y. Fan, A. G. Fitzgerald, P. John, C. E. Troupe, and J. I. B. Wilson, Surf. Interface Anal. **34**, 703 (2002).

[23] A. Hoffman, I. Andrienko, D. N. Jamieson, and S. Prawar, Appl. Phys. Lett. **86**, 044103 (2005).

[24] S. Bhattacharyya, O. Auciello, J. Birrell, J. A. Carlisle, L. A. Curtiss, A. N. Goyette, D. M. Gruen, A. R. Krauss, J. Schlueter, A. Sumant, and P. Zapol, Appl. Phys. Lett. **79**, 1441 (2001).

[25] O. A. Williams, S. Curat, J. E. Gerbi, D. M. Gruen, and R. B. Jackman, Appl. Phys. Lett. **85**, 1680 (2004).

[26] V. Chakrapani, J. C. Angus, A. B. Anderson, S. D. Wolter, B. R. Stoner, and G. U. Sumanaseker, Science **318**, 1424 (2007).

[27] C. E. Nebel, Science **318**, 1391 (2007).